ACI STRUCTURAL JOURNAL TECHNICAL PAPER

Title no. 100-S40

Design Approach for Carbon Fiber-Reinforced Polymer Prestressed Concrete Bridge Beams

by Nabil F. Grace and S. B. Singh

This paper presents a design approach for carbon fiber-reinforced polymer (CFRP) concrete bridge beams prestressed using bonded pretensioning and unbonded post-tensioning tendons arranged in multiple vertically distributed layers along with non-prestressing CFRP rods. Design equations to determine the flexural capacity and to compute the stresses and strains in concrete and tendons are provided. In addition, based on parabolic stress-strain relation for concrete and linear stress-strain relation for tendons, a computer program was developed to compute the overall response of the beam such as deflections, strains, cracking loads, and post-tensioning forces. The design equations and the accuracy of the nonlinear computer program were validated by comparing the analytical results with experimental results from a full-scale double-T (DT) test beam. The difference in the analytical and experimental values of the ultimate moment capacity of the DT-test beam is negligible, whereas the corresponding difference in the ultimate forces in unbonded externally draped post-tensioning strands is approximately 4.1%. A detailed parametric study was conducted to examine the effect of the reinforcement ratio and the level of prestressing forces on the deflections and ultimate load-carrying capacity of the full-scale DT-beam. It is observed that the reinforcement ratio and the level of prestressing have significant effect on the moment-carrying capacity and ultimate load deflection of the beam. The combination of bonded and unbonded prestressing levels (0.3 to 0.6) can significantly increase the ultimate moment capacity of an over-reinforced beam.

Keywords: beam; carbon; ductility; fiber; polymer; prestressed concrete, reinforcement ratio.

INTRODUCTION

With the advent of innovative fiber-reinforced polymer (FRP) materials, the current focus of ongoing worldwide research[1-6] is to gather experimental data, and develop and formulate design guidelines for structures reinforced and prestressed using FRP materials. Due to a lack of uniformity in testing procedures, material characteristics definitions, and reporting procedures, however, there are no suitable guidelines for the design of FRP-reinforced and prestressed concrete beams. Although early testing on FRP materials to develop suitable design guidelines started in Japan, similar research[7-8] in the United States of America and Europe started in the late 1980s. About 5 years ago, Gilstrap et al.[9] presented a comparative evaluation of the previously developed design philosophies. They have referred Canadian, European, and Japanese efforts to codify FRP materials and assess the relative merits of each design approach. Dolan and Burke[10] and Abdelrahman and Rizkalla[11] have examined the flexural behavior of beams partially prestressed using CFRP reinforcements. Most recently, Burke and Dolan[12] have presented an approach for the flexural design of beams prestressed with bonded FRP tendons provided in a single layer. A similar design approach for an under-reinforced beam prestressed with bonded tendons in multiple layers is presented by Dolan and Swanson.[13] From the aforementioned research investigations, it is indicated that there is no unified design approach for the CFRP-reinforced bridge beams prestressed using combined bonded and unbonded CFRP tendons arranged in vertically distributed multiple layers.

In this study, flexural design equations taking into account the effect of multiple layers of bonded pretensioning tendons and unbonded post-tensioning strands, and non-prestressing tendons in tension and compression zones are derived. In addition, a special-purpose, nonlinear computer program was developed that incorporates the design equations developed, taking into account the parabolic stress-strain relationship for concrete and linear stress-strain relationship for CFRP tendons. The accuracy of the program was validated by comparison with an experimentally determined flexural response[14] (considering such response parameters as deflections, forces in unbonded post-tensioning strands, and strains). A parametric study is presented for the double-T (DT) bridge beam (identical to those used in the Bridge Street Bridge[15]) to examine the effect of reinforcement ratio and the level of prestressing on the load-deflection response.

RESEARCH SIGNIFICANCE

In aggressive environments, nonmetallic FRP tendons are considered suitable materials for prestressed concrete structures. The design equations and procedure presented herein will aid the designers in the analysis and design of bridge beams prestressed with bonded pretensioning and unbonded post-tensioning tendons arranged in vertically distributed layers along with non-prestressing tendons in tension and compression zones. Results of the parametric study will provide suitable guidelines for the designers in selecting the appropriate reinforcement ratio and level of prestressing for required design strength and serviceability of the bridge beams.

THEORETICAL DEVELOPMENT OF DESIGN EQUATIONS

The design equations for CFRP-reinforced concrete (RC) beams prestressed with multiple layers of internally bonded and externally unbonded CFRP tendons are developed as follows. These equations are valid for evaluation of the flexural capacity of beams with typical cross sections such as DT, box, and AASHTO-I beam sections. The design is based on balanced ratio,[12,13,16] which characterizes the beam sections

ACI Structural Journal, V. 100, No. 3, May-June 2003.
MS No. 02-146 received April 15, 2002, and reviewed under Institute publication policies. Copyright © 2003, American Concrete Institute. All rights reserved, including the making of copies unless permission is obtained from the copyright proprietors. Pertinent discussion including authors' closure, if any, will be published in the March-April 2004 *ACI Structural Journal* if the discussion is received by November 1, 2003.

ACI member **Nabil F. Grace** *is a professor and Chairman, Civil Engineering Department, Lawrence Technological University, Southfield, Mich. He is a member of ACI Committee 440, Fiber Reinforced Polymer Reinforcement, and Joint ACI-ASCE Committee 343, Concrete Bridge Design. His research interests include the use of advanced composite materials in highway bridges and in the semiconductor construction industry.*

ACI member **S. B. Singh** *is a postdoctoral research scholar in the Civil Engineering Department, Lawrence Technological University. His research interests include carbon fiber-reinforced polymer for reinforcing, prestressing and external strengthening of concrete structures.*

into under-reinforced and over-reinforced sections. Moreover, to predict the overall load versus deflection, strain, and post-tensioning force relationships, a special-purpose, nonlinear computer program was developed incorporating a parabolic stress-strain relationship for concrete and a linear stress-strain relationship for CFRP tendons. The nonlinear computer program is based on computing the resultant compression force in concrete using equivalent rectangular stress block and associated factors, which give the same resultant compression force and its location as obtained using a parabolic stress-strain relationship. Unlike Whitney's stress block factors (ACI 318[17]), these equivalent rectangular stress block factors are not constant but depend on the level of extreme compression fiber strain and type of section. Equations for computing the equivalent rectangular stress block factors corresponding to parabolic stress-strain relationship in concrete are presented later in the section entitled "Nonlinear response."

Definition of material characteristics

The guaranteed ultimate tensile strength, guaranteed rupture strain, and modulus of elasticity of tendons must be specified by the designer and compared against the data provided by the manufacturers. The guaranteed strength[1,18] refers to the mean break strength reduced by three standard deviations. Similarly, the guaranteed rupture strain refers to the mean rupture strain reduced by three standard deviations. The specified guaranteed tensile strength of CFRP tendons is based on at least five test specimens.[1,18]

The following are the basic steps to be followed for the flexural design of prestressed beam with bonded and unbonded CFRP tendons/strands:

1. *Compute the required moment capacity*

Let the dead load moment = M_D, and live load moment = M_L

The required moment capacity of the beam, $M_{required}$ = $1.4M_D + 1.7M_L$ (ACI 318,[17] AASHTO[19]).

2. *Select and proportion the cross section*

Select and proportion the cross section of the beam and specify the number and arrangement of the bonded prestressing tendons, unbonded post-tensioning tendons, and non-prestressing tendons in tension and compression zones. The maximum prestress force in the CFRP tendons should be limited to 65% of the specified tensile strength of tendons.[18,20]

3. *Compute balanced ratio* ρ_b

The balanced ratio is based on strain compatibility in the cross section and signifies the reinforcement ratio at which simultaneous failure of concrete in compression and rupture of the bottom bonded prestressing tendons occurs. This balanced ratio[12] is based on four basic assumptions: a) the ultimate concrete compression strain ε_{cu} is 0.003; b) the nonlinear behavior of concrete is modeled using an equivalent rectangular stress block; c) tendon failure occurs at the ultimate tensile strain of tendon, ε_{fu}; and d) an equivalent prestressing tendon is located at the centroid of multiple layers of prestressing tendons of the same material properties.

$$\rho_b = 0.85\beta_1 \frac{f_c'}{f_{fu}} \frac{\varepsilon_{cu}}{\varepsilon_{cu} + \varepsilon_{fu} - \varepsilon_{pbmi}} \tag{1}$$

where

β_1 = factor defined as the ratio of the depth of equivalent rectangular stress block to the distance from the extreme compression fiber to the neutral axis;

f_c' = specified compressive strength of concrete;

f_{fu} = specified tensile strength of bonded prestressing tendons; and

ε_{pbmi} = initial prestressing strain in bonded prestressing tendons of m-th row (bottom row).

Note that the aforementioned balanced ratio is based on material properties of bonded prestressing tendons with the assumption that bonded prestressing tendons are susceptible to early failure. It should also be noted that unlike the balanced ratio for steel, the balanced ratio for FRP bars/tendons does not signify the yielding, but rather, the failure/rupture of bars. Hence, there is no reserve strength of FRP bars/tendons beyond rupture. Limiting the initial effective prestressing strain in FRP tendons, however, can provide an appropriate safety margin against creep and rupture of tendons under service load conditions. Herein, the actual reinforcement ratio of the section is defined as the ratio of the total weighted cross-sectional area of tendons to the effective concrete cross-sectional area. The weighting factor α_i is defined as the ratio of the stress in a particular equivalent tendon (that is, a tendon located at the centroid of tendons of the same material and having the cross-sectional area equal to the total cross-sectional area of corresponding tendons) at the balanced condition to the specified ultimate strength of bonded pretensioning tendons. Herein, the balanced condition refers to the condition at which crushing of concrete and rupture of the bottom pretensioning tendons occurs simultaneously. The following expression should be used for calculating the reinforcement ratio. This expression is obtained using equilibrium of forces and compatibility of strains in the cross section.

$$\rho = \frac{\sum_{i=1}^{p} A_{fi}\alpha_i}{bd_m} \tag{2}$$

$$= \frac{\sum_{i=1}^{m} F_{pi} + f_{pbb}A_{pb} + f_{pnbb}A_{pn} + F_{pui} + f_{pub}A_{fu} - f_{pnfb}A_{pnf}}{b \times d_m \times f_{fu}}$$

where

α_i = f_{bi}/f_{fu};

A_{fi} = cross-sectional area of reinforcement of a particular material (A_{fi} is positive for tensile reinforcement and negative for compression reinforcement);

A_{fu} = total cross-sectional area of post-tensioning tendons;

A_{pb} = total cross-sectional area of pretensioning bonded tendons;

A_{pn} = total cross-sectional area of non-prestressing tendons located in webs;

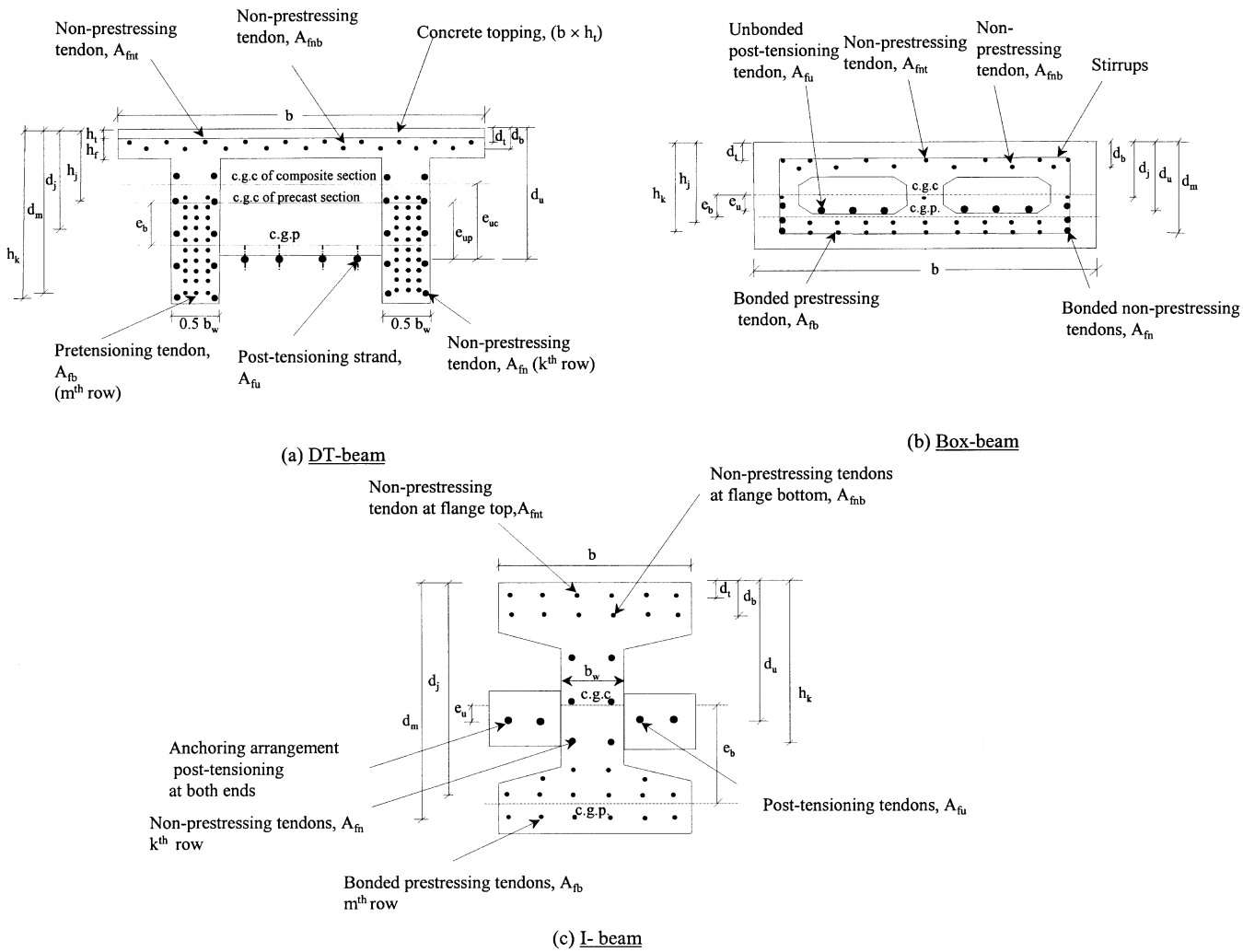

Fig. 1—Typical cross sections for bridge beams with bonded and unbonded tendons.

A_{pnf} = total cross-sectional area of non-prestressing tendons in flange;

b = flange width of the beam;

d_m = distance of centroid of bottom prestressing tendons from the extreme compression fiber;

f_{bi} = total stress in an equivalent tendon of a specific material at the balanced condition;

f_{pbb} = flexural stress in the equivalent bonded pretensioning tendons at the balanced condition:

f_{pnbb} = flexural stress in the equivalent non-prestressing tendons of webs at the balanced condition:

f_{pnfb} = flexural stress in the equivalent non-prestressing tendons of flange at the balanced condition;

f_{pub} = flexural stress in the equivalent unbonded tendons at the balanced condition;

$\sum_{j=1}^{m} F_{pi}$ = resultant initial effective pretensioning force;

F_{pui} = resultant initial effective post-tensioning force;

m = total number of layers of bonded pretensioning tendons; and

p = total number of reinforcing materials.

4. *Compute cracking moment* M_{cr} *of section*

The cracking moment can be determined using the concept that stress in the extreme tensile fiber of the prestressed section under the superimposed moment (equal to cracking moment) should be equal to the modulus of rupture f_r of concrete.[21]

$$M_{cr} = (f_r + \Sigma\sigma_{bp})S_b \tag{3}$$

where

f_r = $6.0\sqrt{f_c'}$ (ACI 318[17])

$\Sigma\sigma_{bp}$ = resultant stress at extreme tension fiber of the beam due to effective pretensioning and post-tensioning forces; and

S_b = section modulus corresponding to the extreme tension fiber.

5. *Calculate flexural capacity*

The flexural capacity of the DT-beam, box-beam, and AASHTO-I beam provided with prestressing bonded and unbonded tendons arranged in vertically distributed multiple layers and classified as significantly under-reinforced, under-reinforced, and over-reinforced beams can be determined using the following approach. These beams are used in the construction of prestressed concrete bridges. Figure 1 shows the typical DT-beam, box-beam, and AASHTO-I beam sections with tendons arranged in vertically distributed multiple layers.

A. *Significantly under-reinforced beams*—The reinforcement ratio ρ of significantly under-reinforced beams lies below

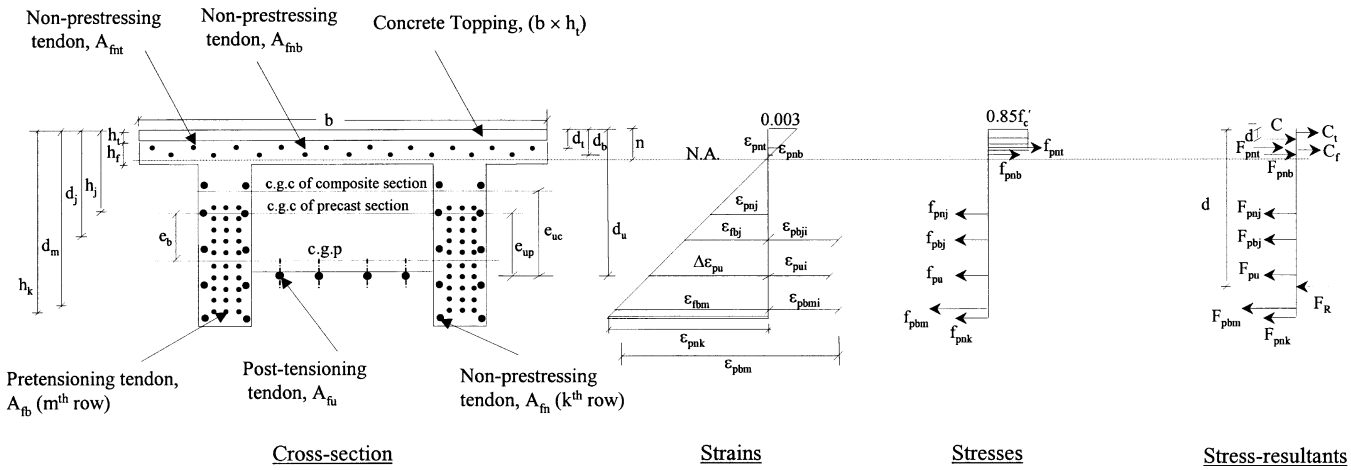

Fig. 2—Strain and stress distributions for over-reinforced beam at ultimate.

$0.5\rho_b$ (Burke and Dolan[12]). The failure of such beams will occur due to the rupture of the bottom prestressing tendons. The compressive stress distribution at ultimate for a typical significantly under-reinforced DT-beam will be triangular because compressive stresses in such a section will be within the linear elastic range. The strain distribution will be similar to that shown in Fig. 2 for the over-reinforced beam, except that the strain in the bottom prestressing tendon will be equal to specified rupture strain for prestressing tendons.

Assume that there are m rows of pretensioning tendons and k rows of non-prestressing tendons arranged vertically in the webs of the DT-beam, box-beam, and AASHTO-I beam sections. The first row lies at the top, while the m-th and k-th rows lie near the bottom of beams.

The depth to neutral axis is defined as $n = k_u d_m$, where coefficient k_u for the significantly under-reinforced section is defined by Eq. (4). This equation is derived using compatibility and equilibrium equations.

$$k_u = \frac{-B + \sqrt{B^2 - 4AC}}{2A} \tag{4}$$

where

$$A = \frac{bd_m^2}{2} f_{fu}\left(1 - \frac{f_{pbmi}}{f_{fu}}\right)\frac{E_c}{E_f};$$

$$B = \left[F_{pe} d_m + \varepsilon_f d_m \left(\sum_{i=1}^{q} A_{fi}E_{fi} + \Omega_c A_{fu}E_{fp}\right)\right]$$

$$C = -\left[F_{pe} d_m - \varepsilon_f \left(\sum_{i=1}^{q} A_{fi}E_{fi}h_i + \Omega_c A_{fu}E_{fp}d_u\right)\right]$$

A_{fi} = cross-sectional area of bonded tendons in a particular layer (it is negative for tendons in compression zone);
b = flange width of beam;
d_m = distance from the extreme compression fiber to the centroid of the bottom prestressing tendons;
f_{pbmi} = initial effective prestress in bottom bonded prestressing tendons (m-th row)
F_{pe} = total initial effective pre-tensioning and post-tensioning force;
E_{fi} = modulus of elasticity of bonded tendons in a particular layer;
E_{fp} = modulus of elasticity of unbonded strands;
h_i = distance of bonded tendons of an individual layer from the extreme compression fiber;
ε_f = difference in ultimate rupture strain and initial prestressing strain of bottom prestressing tendons;
q = number of layers of bonded tendon; and
Ω_c = bond reduction coefficient for elastic cracked section (Naaman and Alkhairi[22])
= $\Omega(I_{cr}/I_{tr})$

where

Ω = bond reduction coefficient for elastic uncracked section (Naaman and Alkhairi[22])
= 1/2 for one-point loading
= 2/3 for two-point loading or uniform loading;
I_{tr} = gross transformed moment of inertia of cross section; and
I_{cr} = gross transformed moment of inertia of cracked section.

Note that bond reduction coefficients are introduced to take into account the lower strain in unbonded tendons with respect to equivalent bonded tendons (Naaman and Alkhairi[22]). Also, it is assumed that the section is not cracked under the service load condition. The following steps are taken to compute the moment-carrying capacity of the beam.

i. Compute strains in bonded tendons and concrete

Strain in prestressing tendons of an individual row,

$$\varepsilon_{pbj} = (\varepsilon_{fu} - \varepsilon_{pbmi})\frac{(d_j - n)}{(d_m - n)} + \varepsilon_{pbji} \quad (\text{for } j = 1, m)$$

Strain in non-prestressing tendons of an individual row,

$$\varepsilon_{pnj} = (\varepsilon_{fu} - \varepsilon_{pbmi})\frac{(h_j - n)}{(d_m - n)} \quad (\text{for } j = 1, k)$$

Strain in non-prestressing tendons of flange top,

$$\varepsilon_{pnt} = (\varepsilon_{fu} - \varepsilon_{pbmi})\frac{(n - d_t)}{(d_m - n)}$$

Strain in non-prestressing tendons of flange bottom,

$$\varepsilon_{pnb} = (\varepsilon_{fu} - \varepsilon_{pbmi})\frac{(n - d_b)}{(d_m - n)}$$

Strain in concrete at the extreme compression fiber,

$$\varepsilon_c = (\varepsilon_{fu} - \varepsilon_{pbmi})\frac{n}{(d_m - n)}$$

where

d_j = depth from extreme compression fiber to the centroid of prestressing tendons of an individual row;

h_j = depth from extreme compression fiber to the centroid of non-prestressing tendons of an individual row;

h_k = depth from extreme compression fiber to the centroid of bottom non-prestressing tendons;

d_b = depth from extreme compression fiber to the centroid of non-prestressing tendons at the bottom of flange;

d_t = depth from extreme compression fiber to the centroid of non-prestressing tendons at the top of flange;

n = depth to the neutral axis from the extreme compression fiber;

ii. Compute strains in unbonded post-tensioning tendons

Strain in the unbonded post-tensioning tendons,

$$\varepsilon_{pu} = \varepsilon_{pui} + \Delta\varepsilon_{pu}$$

$$\Delta\varepsilon_{pu} = \Omega_c \frac{(\varepsilon_{fu} - \varepsilon_{pbmi})(d_u - n)}{(d_m - n)}$$

iii. Compute stresses in tendons

Stress in bonded prestressing tendons of an individual row,

$f_{pbj} = E_f \times \varepsilon_{pbj} \le f_{fu}$

Stress in unbonded post-tensioning tendons,

$f_{pu} = E_{fp} \times \varepsilon_{pu} \le f_{fup}$

Stress in non-prestressing tendons of an individual row,

$f_{pnj} = E_{fn} \times \varepsilon_{pnj} \le f_{fun}$

Stress in non-prestressing tendons at flange top,

$f_{pnt} = E_f \times \varepsilon_{pnt} \le f_{fu}$

Stress in non-prestressing tendons at flange bottom,

$f_{pnb} = E_f \times \varepsilon_{pnb} \le f_{fu}$

iv. Compute resultant forces in tendons

Resultant force in bonded prestressing tendons of each row,

$F_{pbj} = f_{pbj} \times A_{fb}$

Resultant force in unbonded post-tensioning tendons,

$F_{pu} = f_{pu} \times A_{fu}$

Resultant force in non-prestressing tendons of each row,

$F_{pnj} = f_{pnj} \times A_{fn}$

Resultant force in non-prestressing tendons at flange top,

$F_{pnt} = f_{pnt} \times A_{fnt}$

Resultant force in non-prestressing tendons at flange bottom,

$F_{pnb} = f_{pnb} \times A_{fnb}$

where

A_{fb} = total cross-sectional area of bonded prestressing tendons in each row;

A_{fn} = total cross-sectional area of non-prestressing tendons in each row;

A_{fnt} = total cross-sectional area of compression non-prestressing tendons at flange top;

A_{fnb} = total cross-sectional area of compression non-prestressing tendons at flange bottom; and

A_{fu} = total cross-sectional area of unbonded tendons.

v. Compute ultimate moment-carrying capacity

Let the centroid of the resultant (F_R) of tensile forces F_{pbj} (for $j = 1, m$), F_{pnj} (for $j = 1, k$), and F_{pu} lies at a distance d and the centroid of resultant compression force (C_R) lies at a distance $\overline{d}$ from the extreme compression fiber. Here, resultant compression force comprises of compression force in concrete and compression reinforcement. Nominal moment of resistance M_n is expressed as follows

$$M_n = F_R\,(d - \overline{d}) \tag{5}$$

where

$$F_R = \sum_{j=1}^{m} F_{pbj} + \sum_{j=1}^{k} F_{pnj} + F_{pu} \tag{6}$$

The design moment capacity M_u is expressed as

$$M_u = \phi M_n \tag{7}$$

where

ϕ = strength reduction factor; and

ϕ = 0.85 for CFRP tendons (Burke and Dolan[12] and CHBDC[23]).

vi. Compare design moment capacity and required moment capacity

$$M_u \ge M_{required}, \text{ that is, } \phi M_n \ge M_{required} \tag{8}$$

vii. Check for stresses in concrete

$$f_c = f_{fu}\left(1 - \frac{f_{pbmi}}{f_{fu}}\right)\left(\frac{n}{d_m - n}\right)\frac{E_c}{E_f} \tag{9}$$

E_c = modulus of elasticity of concrete; and

f_{pbmi} = initial effective prestress in the bottom tendons.

$$f_c = \varepsilon_c \times E_c \le 0.40 f_c' \text{ (Tan et al.[24])} \tag{10}$$

where E_c can be taken as equal to $57{,}000\sqrt{f_c'}$ psi (ACI 318[17]) in the absence of experimental results. If $f_c \ge 0.40\, f_c'$, then the moment capacity of beam should be calculated as per the procedure outlined as follows for an under-reinforced beam.

B. *Under-reinforced beams*—The reinforcement ratio ρ of under-reinforced beams lies between $0.5\rho_b$ and ρ_b (Burke and Dolan[12]). In this class of beams, the rupture of bottom prestressing tendons governs failure. Unlike significantly under-reinforced beams, however, the stress in the concrete at failure of under-reinforced beams will be within the nonlinear range. The concrete stress distribution can be approximated by Whitney's rectangular stress block (Fig. 2). The strain distribution will be similar to that for the significantly under-reinforced beam. The depth to the neutral axis ($n = k_u d_m$) of under-reinforced beam can obtained using coefficient k_u defined by

$$k_u = \frac{-B \pm \sqrt{B^2 - 4AC}}{2A} \quad (11)$$

where

$A = 0.85 f_c' b \beta_1 d_m^2$

$$B = -\left[A + F_{pe} d_m + \varepsilon_f d_m \left(\sum_{i=1}^{q} A_{fi} E_{fi} + \Omega_u A_{fu} E_{fp}\right)\right]$$

$$C = \left[F_{pe} d_m + \varepsilon_f \left(\sum_{i=1}^{q} A_{fi} E_{fi} h_i + \Omega_u A_{fu} E_{fp} d_u\right)\right]$$

i. Compute strains and stresses

The strains, stresses, forces in bonded tendons, and moment capacities are calculated in the same manner as for significantly under-reinforced beams. Computation of strains and stresses in the unbonded tendon, however, is based on the ultimate bond reduction coefficient Ω_u due to nonlinearity of stress and strain relationship in the concrete. The resultant compressive force in concrete is computed using Whitney's equivalent rectangular stress block. The compression force resultants corresponding to concrete topping and flange of precast section are expressed by Eq. (12) and (13), respectively. These compression force resultants are added to resultant forces in compressive reinforcements to get resultant compressive force of the section.

$$C_t = 0.85 f_c' \frac{E_{ct}}{E_c} h_t b \quad (12)$$

$$C_f = 0.85 f_c' b(\beta_1 n - h_t) \quad (13)$$

The ultimate bond reduction coefficient (Naaman and Alkhairi[22]) is expressed as follows

$\Omega_u = 2.6/(L_u/d_u)$ for one-point loading

$= 5.4/(L_u/d_u)$ for two-point loading or uniform loading

where

L_u = horizontal distance between the ends of the post-tensioning strands.

C. *Over-reinforced beams*—For over-reinforced beams, reinforcement ratio ρ is greater than balanced ratio ρ_b (Burke and Dolan[12]). The failure of over-reinforced beams is governed by the crushing of concrete in the compression zone. The stress in the concrete at failure will be in the nonlinear range and hence, the stress distribution can be approximated by Whitney's rectangular stress block (Fig. 2). In over-reinforced sections, the depth to the neutral axis ($n = k_u d_m$) can be determined using the coefficient k_u defined in Eq. (14). This coefficient is derived using equilibrium and compatibility equations for the section.

$$k_u = \frac{A + \sqrt{A^2 + 4B}}{2} \quad (14)$$

where

$$A = \frac{\left[\left(\sum_{j=1}^{m} A_{fb} E_f \varepsilon_{pbji} + A_{fu} \varepsilon_{pui} E_{fp}\right) - \varepsilon_{cu}\left(\sum_{j=1}^{q} A_{fj} E_{fj} + \Omega_u A_{fu} E_{fp}\right)\right]}{0.85 f_c' b \beta_1 d_m}$$

$$B = \frac{\varepsilon_{cu}\left(\sum_{j=1}^{q} A_{fj} E_{fj} h_j + \Omega_u A_{fu} E_{fp} d_u\right)}{0.85 f_c' b \beta_1 d_m^2}$$

A_{fj} = cross-sectional area of prestressing or non-prestressing bonded tendons in an individual row;

E_{fj} = modulus of elasticity of bonded tendons of an individual row;

h_j = distance of bonded tendons from the extreme compression fiber; and

q = total number of layers of bonded prestressing and non-prestressing tendons.

i. Compute strains in tendons

Strain in bonded prestressing tendons,

$\varepsilon_{pbj} = (0.003/n)(d_j - n) + \varepsilon_{pbji}$ (for $j = 1, m$)

Strain in non-prestressing tendons,

$\varepsilon_{pnj} = (0.003/n)(h_j - n)$ (for $j = 1, k$)

Strain in non-prestressing tendons at flange top,

$\varepsilon_{pnt} = (0.003/n)(n - d_t)$

Strain in non-prestressing tendons at flange bottom,

$\varepsilon_{pnb} = (0.003/n)(n - d_b)$

Strain in unbonded tendons,

$\varepsilon_{pu} = \varepsilon_{pui} + \Delta\varepsilon_{pu}$

$= \varepsilon_{pui} + \Omega_u(0.003/n)(du - n)$

It is to be noted that the stresses and forces in tendons and concrete, and nominal and required moment capacities of the section can be calculated in the similar manner as for under-reinforced beams.

DEFLECTION AND STRESSES UNDER SERVICE LOAD CONDITION

Assuming that the service live load is applied through two-point loading system, the maximum beam deflection and tendon stresses prior to cracking load can be computed using the expressions given below:

Deflection due to applied load,

$$\delta_a = \frac{M_L L_1^2}{8 E_c I_c}\left[\frac{8}{3} + 4\left(\frac{L_2}{L_1}\right) + \left(\frac{L_2}{L_1}\right)^2\right] \downarrow$$

Deflection due to dead load,

$$\delta_d = \frac{5 \ W_d L^4}{384 E_c I_c} \downarrow$$

Deflection due to prestressing forces,

$$\delta_p = \frac{L^2}{8 E_c I_c}\left[F_{pre} \ e_b + F_{post} \ e_{uc}\left(\frac{L_u}{L}\right)^2\right] \uparrow$$

Net downward deflection of the beam,

$$\delta = \delta_a + \delta_d - \delta_p \downarrow$$

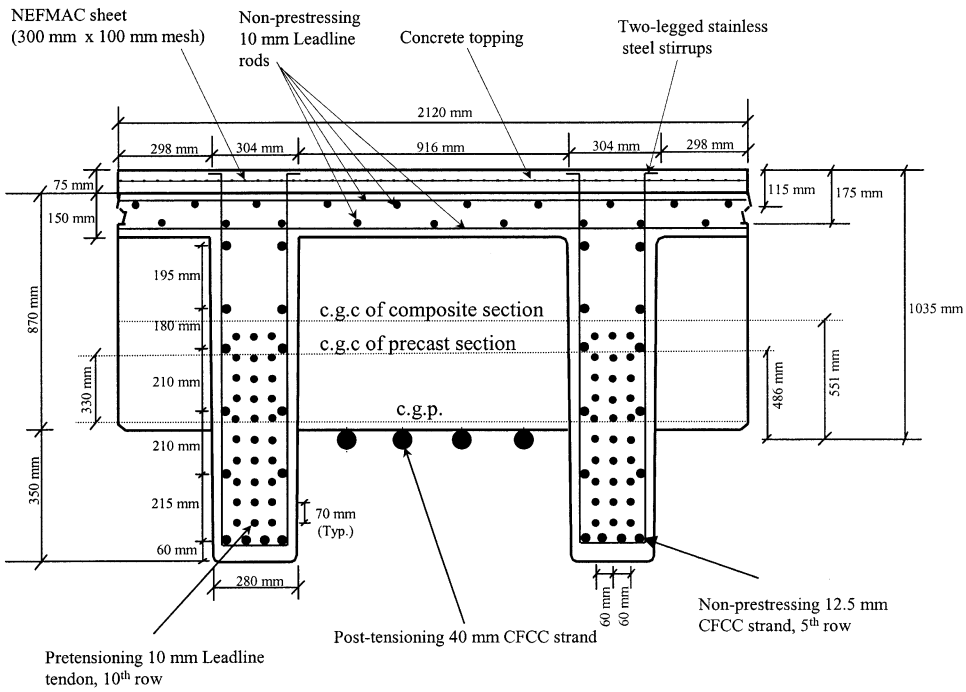

Fig. 3—Cross section of full-scale DT beam at midspan.

Stress in a bonded tendon of individual layer,

$$f_{pbj} = E_f \varepsilon_{pbj} + \frac{E_f}{E_c} \frac{M(d_j - y_{tc})}{I_c}$$

Stress in unbonded tendon,

$$f_{pu} = E_{fp} \varepsilon_{pui} + \frac{E_{fp}}{E_c} \frac{(M - M_D)}{I_c} \Omega$$

Stress in non-prestressing tendons,

$$f_{pn} = \frac{E_{fn}}{E_c} \frac{M(h_j - y_{tc})}{I_c}$$

where

L_1 = distance between support and nearest load point;
L_2 = longitudinal distance between two load points;
L = effective span of the beam;
M_L = service live load moment;
e_b = eccentricity of resultant pretensioning force from the centroid of precast section;
e_{uc} = eccentricity of unbonded tendons from the centroid of composite section; and
I_c = moment of inertia of composite cross section of beam (precast section plus concrete topping).

NONLINEAR RESPONSE

The response of the beam under service load condition and before cracking can be determined using simple linear elastic beam theory. However, to predict the overall response of the beam from the onset of cracking of the section to the ultimate failure, a nonlinear analysis is required. The non-linear stress and strain relationship for concrete can be modeled by the expression given in Eq. (15). Similar parabolic stress strain relationship for concrete was assumed by Tan, Abdullah-Al Farooq, and Ng[24] except that they have taken ε_{cu} equal to 0.002. In the present investigation, however, ε_{cu} has been taken as 0.003 as per the recommendation of ACI 318.[17]

$$\frac{f_c}{f_c'} = 2\frac{\varepsilon_c}{\varepsilon_{cu}} - \left(\frac{\varepsilon_c}{\varepsilon_{cu}}\right)^2 \tag{15}$$

where

f_c = stress in concrete corresponding to strain ε_c.

The resultant compressive force in concrete based on a nonlinear stress-strain relation can be computed using equivalent rectangular stress block factors at any load stage. The stress block factors can be determined by equating the resultant compression force and its location obtained from nonlinear stress-strain relation to that obtained by equivalent stress block. Equation (16) expresses the resultant compression force, while Eq. (17) can be used to locate the centroid of resultant compression force.

$$\int_0^n f_c b\,dy = \alpha f_c' \beta n b \tag{16}$$

$$\bar{y}_c = \frac{\int_0^n f_c b y\,dy}{\int_0^n f_c b\,dy} \tag{17}$$

Using Eq. (15) to (17), the stress block factors for rectangular and flanged sections can be obtained using following expressions:

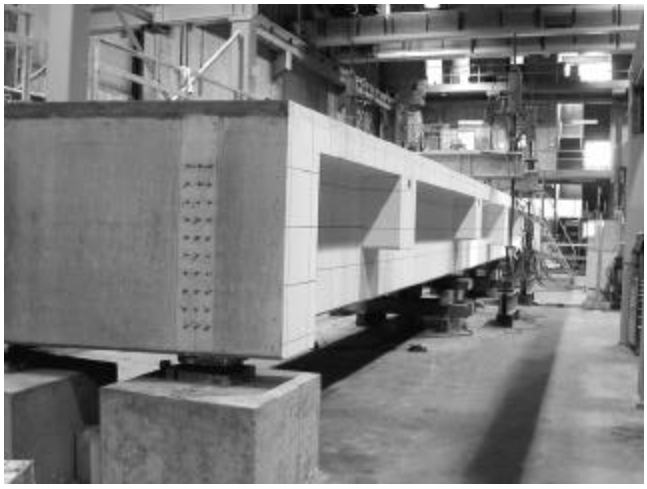

Fig. 4—Test setup for flexural loading.

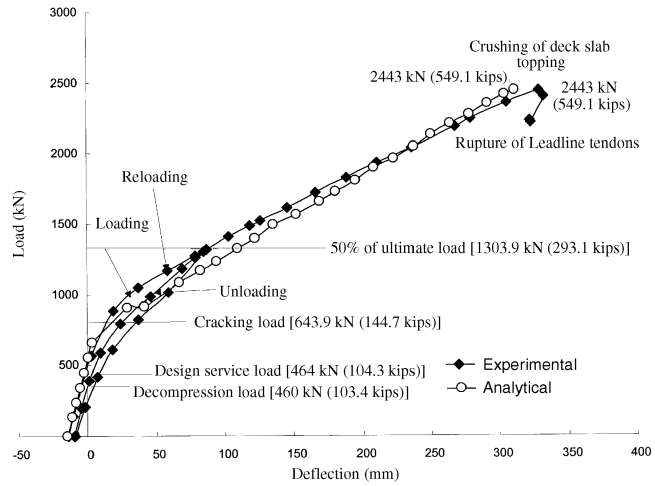

Fig. 5—Midspan deflection response of full-scale DT beam.

Rectangular section: For a rectangular section, stress block factors (α_1, β_1) are evaluated using Eq. (18a) and (18b)

$$\alpha_1\beta_1 = \frac{\varepsilon_t}{\varepsilon_{cu}} - \frac{1}{3}\left(\frac{\varepsilon_t}{\varepsilon_c}\right)^2 \tag{18a}$$

$$\beta_1 = \frac{4 - \dfrac{\varepsilon_t}{\varepsilon_{cu}}}{6 - \dfrac{2\varepsilon_t}{\varepsilon_{cu}}} \tag{18b}$$

where

ε = strain at the extreme compression fiber at a specific stage of loading.

Flanged section: For a flanged section, the corresponding stress block factors (α_2, β_2) can be calculated using the following expressions

$$\alpha_2 = \frac{A1}{d_f b + (\beta_2 n - d_f) b_w} \tag{19a}$$

where

$$A1 = \frac{\varepsilon_t}{n\varepsilon_{cu}}[(n-d_f)^2(b_w-b) + bn^2]$$

$$-\frac{1}{3}\left(\frac{\varepsilon_t}{n\varepsilon_{cu}}\right)^2[(n-d_f)^3(b_w-b) + bn^3]$$

and β_2 can be evaluated by solving the following quadratic equation

$$\beta_2^2\frac{b_w n^2}{2} - \beta_2\left(b_w - n^2\frac{B1}{A1}b_w n\right) \tag{19b}$$

$$-d_f\left[\left(n - \frac{d_f}{2} - \frac{B1}{A1}\right)(b - b_w)\right] = 0$$

where

$$B1 = \frac{2}{3}\frac{\varepsilon_t}{n\varepsilon_{cu}}[(n-d_f)^3(b_w-b) + bn^3]$$

$$-\frac{1}{4}\left(\frac{\varepsilon_t}{n\varepsilon_{cu}}\right)^2[(n-d_f)^4(b_w-b) + bn^4]$$

Using the linear elastic theory for computation of linear response and nonlinear stress-strain relation of concrete for the nonlinear response, a computer program was developed for predicting the overall load versus deflections, strains, stresses, forces in bonded and unbonded tendons, and moment curvature relationships. The nonlinear response is based on the incremental strain controlled approach, wherein equilibrium of forces is achieved for each level of compressive concrete strain and corresponding tensile strain. The calculation of deflection is based on numerical integration of curvatures along the length of beam.

EXPERIMENTAL VERIFICATION

To evaluate the accuracy of results predicted by the developed special-purpose, nonlinear computer program, analytical results were compared with experimental results[14] conducted on a full-scale DT-beam. The cross section of the DT-beam tested is given in Fig. 3, while the test setup for the DT-beam is shown in Fig. 4. The total span of the test beam was 20.4 m (67 ft). A four-point loading system was used with a 3.658 m (12 ft) center-to-center distance between two parallel cross-heads. The distance between the crosshead and the nearest beam support was 8.382 m (27.5 ft). The experimental and analytical results for the full-scale DT-test beam are compared in Fig. 5 to 7.

As shown in Fig. 5, the analytical load-versus-deflection curve is very close to that of the experimental curve from the beginning of the loading to ultimate failure of the full-scale DT-beam. Also, it is worth noting that the analytical and experimental load-carrying capacities of the beam are almost the same (2443 kN). Since the experimentally observed ultimate failure strain of concrete topping[14] was 0.0025, the analytical failure load also corresponds to the same strain level. As mentioned previously, the nonlinear response was predicted using incremental strain controlled approach,

Table 1—Characteristics of CFRP tendons/ CFCC strands

Characteristics	Tendons (MCC[25])	CFCC 1 x 7 (Tokyo Rope[26])	CFCC 1 x 37 (Tokyo Rope[26])
Nominal diameter, mm (in.)	10 (0.39)	12.5 (0.5)	40 (1.57)
Effective cross-sectional area, mm^2 ($in.^2$)	71.6 (0.111)	76.0 (0.118)	752.6 (1.17)
Guaranteed tensile strength, kN/mm^2 (ksi)	2.26 (328)	1.87 (271)	1.41 (205)
Specified tensile strength* kN/mm^2 (ksi)	2.86 (415)	2.10 (305)	1.87 (271)
Young's modulus of elasticity, kN/mm^2 (ksi)	147 (21,320)	137 (19,865)	127 (18,419)
Elongation, %	1.9	1.5	1.5
Guaranteed breaking load, kN (kips)	162 (36.4)	142 (31.9)	1070 (240.5)
Ultimate breaking load, kN (kips)	204.7 (46)	160 (36)	1410 (316.9)

*Ultimate tensile strength characteristics of tendons and strands were obtained from test, whereas manufacturers supplied other properties.

wherein applied load was predicted corresponding to each strain level using equilibrium equations. Similarly, it is observed from Fig. 6 that, like deflection, the analytical value of the unbonded post-tensioning strand forces are almost identical to the corresponding experimental values in the precracked and early postcracking stage of the beam. In the advanced post-cracking stage, however, the analytical values of the post-tensioning forces are slightly lower in comparison to the corresponding experimental values. The maximum difference in the analytical and experimental unbonded post-tensioning forces occurs at the ultimate failure of the beam and is equal to 4.1%. In Fig. 5 and 6, decompression load refers to the load at which all the precompression in tension zone is lost and at which no further increase in the strain (at the location of the first crack) occurs. This load was experimentally determined by the load-versus-strain (near the first crack) diagram. This is used to determine the effective prestress in the pretensioning tendons.

Figure 7 shows the load-versus-strain relationships for the strain at the concrete topping. In the figure, tensile strains are shown as positive and compressive strains are shown as negative. It is observed that the analytical and experimental loads versus compressive strain curves at the top of the beam are almost identical and very close to each other.

PARAMETRIC STUDY

To examine the effect of the reinforcement ratio and the level of prestressing on the flexural response of beam, a detailed parametric study was conducted using the developed, nonlinear, special-purpose computer program for the DT-test beam (Fig. 3 and 4). The material properties of the CFRP tendons,[25] CFCC strands,[26] sheets,[27] and concrete used in the DT-beam are presented in Table 1, 2, and 3, respectively. It should be noted that the specified ultimate strength characteristics of tendons and strands are based on the test results, while manufacturers supplied the other properties of tendons and strands. The properties of precast concrete, concrete topping, and sheets are based on the test results. The parametric results are presented and discussed in the following sections.

Effect of reinforcement ratio

The load-versus-deflection relationships of the DT-beam for different reinforcement ratios are shown in Fig. 8. The

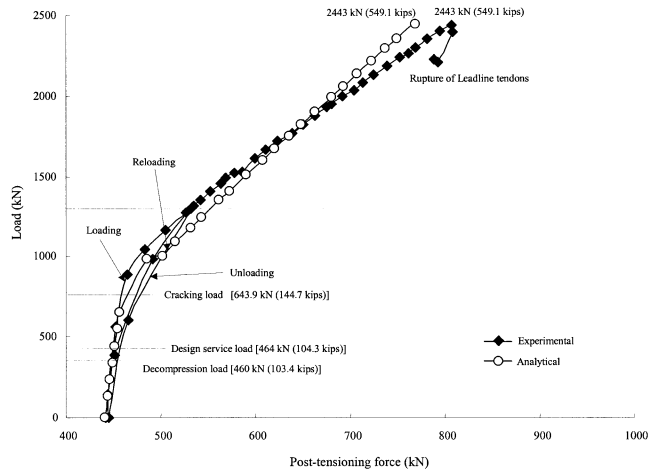

Fig. 6—Force in one of post-tensioning external strands of full-scale DT beam.

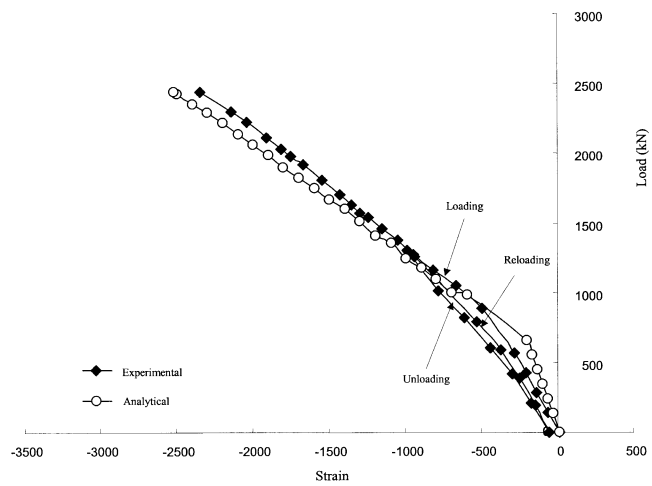

Fig. 7—Strain response at concrete topping of full-scale DT beam.

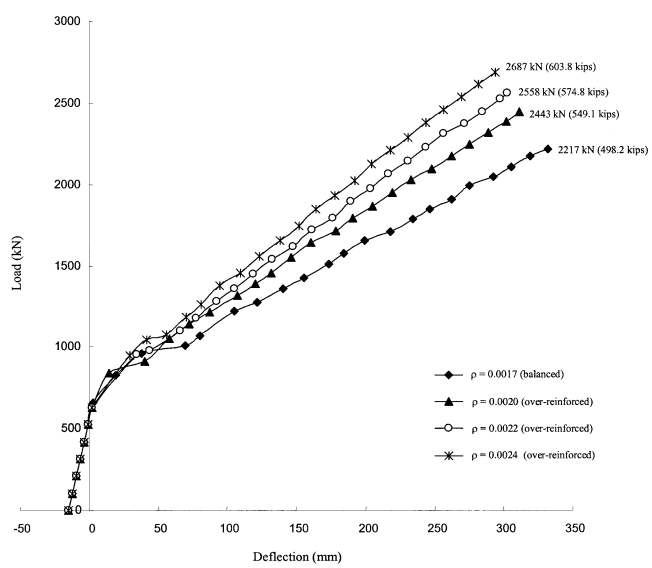

Fig. 8—Effect of reinforcement ratio on load-deflection response of full-scale DT beam.

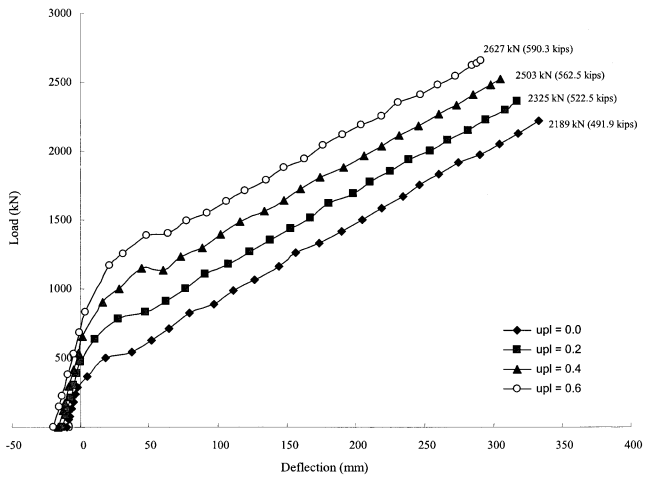

Fig. 9—Load-versus-deflection relationships of full-scale DT beam for different unbonded prestressing levels with constant bonded prestressing level, bpl = 0.41, and reinforcement ratio $\boldsymbol{r}$ *= 0.002.*

reinforcement ratio refers to the total cross-sectional area of prestressing and non-prestressing tendons expressed in terms of equivalent tendons, while keeping the level of bonded prestressing (bpl)* and unbonded prestressing forces (upl)† constants (that is, bpl = 0.41 and upl = 0.31). While varying the reinforcement ratio, the locations of tendons/strands were kept the same and only the cross-sectional area and material properties of tendons were changed based on commercially available tendons[25] and CFCC strands.[26] It is shown that there is no significant effect of the reinforcement ratio on the deflection of the beam in the pre- and early postcracking stages. In the advanced postcracking stage of the beam, however, deflection is significantly affected by the reinforcement ratio. It is observed that for a specific load, deflection is higher for a lower reinforcement ratio. The deflection corresponding to the zero load represents upward camber of the beam. Note that the reinforcement ratio of 0.0017 corresponds to a balanced beam, while other reinforcement ratios (0.0020, 0.0022, and 0.0024) represent over-reinforced beams. It should also be noted that, unlike steel reinforced beams, over-reinforced beams using CFRP reinforcements have better ductility characteristics in comparison to that of under-reinforced beams. Hence, in the case of CFRP reinforced beams, over-reinforced sections are desirable instead of under-reinforced sections.

Effect of level of prestressing

Figure 9 shows the load-versus-deflection response for different unbonded prestressing force levels (upl = 0.0 to 0.6) with a constant bonded prestressing force level (bpl = 0.41). In the figure, zero level of unbonded prestressing refers to the zero initial prestressing force in the existing post-tensioning strands. It is observed that, for a specific load, deflection is higher for lower level of prestressing in comparison to that for the higher level of prestressing. It should be noted that the higher level of unbonded prestressing force will result in the higher energy ratio (ratio of inelastic energy absorbed in the beam to the total energy of the beam) for the over-reinforced DT-beam (ρ = 0.002) and hence, the better ductility of the beam. The energy ratios are observed to be higher for a CFRP over-reinforced beam failing due to crushing of concrete. Hence, the crushing of concrete is a desirable mode of failure for a CFRP-reinforced concrete beam.

*Bonded prestressing force level (bpl) refers to the ratio of total initial prestressing stress to the specified tensile strength of bonded tendons.

†Unbonded prestressing force level (upl) refers to the ratio of total initial prestressing stress to the specified tensile strength of unbonded post-tensioning strands.

Table 2—Characteristics for sheets[27]*

Modulus of elasticity, GPa (ksi)	86.5 (12,540)
Ultimate strength, MPa (ksi)	1500 (217)
Ultimate strain, %	1.8

*Material characteristics of sheets were predicted from test results.

Table 3—Characteristics* of precast concrete and concrete topping

Characteristics	Precast concrete	Concrete topping
Modulus of elasticity, GPa (ksi)	36.7 (5320)	31.6 (4580)
Strength, MPa (ksi)	53.8 (7.81)	39.3 (5.7)

*Characteristics of precast concrete and concrete topping are based on test results.

CONCLUSIONS

Based on the present investigation on the CFRP-reinforced beam prestressed with bonded pretensioning CFRP tendons arranged in vertically distributed multiple layers and unbonded external draped post-tensioning CFCC strands, the following conclusions can be drawn:

1. Design equations derived herein predict concrete strains, post-tensioning forces in unbonded strands, moment-carrying capacity, and deflection of the beam that are in close agreement with the experimental values. The analytical and experimental values of the ultimate moment capacity of the DT-beam are almost the same, while the maximum difference (4.1%) in the experimental and analytical values of post-tensioning forces occurs at the ultimate beam failure;

2. Design equations will aid the designers to accurately and easily estimate the forces in bonded and unbonded tendons, and flexural capacity of bridge beams of various sections such as DT-section, box-section, and AASHTO-I beam section reinforced with tension and compression non-prestressing tendons and prestressed with bonded and unbonded prestressing tendons with any combination of material characteristics of tendons and concrete;

3. The reinforcement ratio has significant effect on the deflection, moment capacity, and forces in unbonded post-tensioning strands;

4. For a specific load, deflection is higher for the lower reinforcement ratio and for the lower prestressing force level in comparison to that for the higher reinforcement ratio, and higher prestressing force level, respectively. The load-versus-deflection curves can be utilized to obtain the deflection of the beam corresponding to the service load, cracking load, and ultimate load of the beam to ensure the serviceability condition of the beam; and

5. The ductility of the beam is improved due to increase in the level of prestressing. The combination of bonded and unbonded prestressing levels (0.3 to 0.6) can significantly increase the moment-carrying capacity and ductility of the over-reinforced beam.

ACKNOWLEDGMENTS

The full-scale DT test beam was constructed by the Prestressed System Inc. (PSI), Windsor, Ontario, Canada and tested by the Construction Technology

Laboratory Inc. (CTL), Skokie, Ill. The design approach presented in this paper has been supported by a grant (CCMS00940391) from the National Science Foundation. The Federal Highway Administration and the City of Southfield funded the experimental work. Hubell, Roth & Clark (HRC) Consulting Engineers, Bloomfield Hills, Mich. provided the design details and the construction drawings. The contributions of F. C. Navarre and R. B. Nacey of HRC and L. Collavino of the Prestressed System Inc. in the construction and testing of the DT beam are gratefully acknowledged.

NOTATION

A_c = cross-sectional area of composite DT-beam
A_{fb} = cross-sectional area of bonded prestressing tendons in each row
A_{fi} = cross-sectional area of tension reinforcement of particular material
A_{fn} = cross-sectional area of non-prestressing tendons in each row
A_{fnb} = cross-sectional area of non-prestressing tendons at bottom of flange
A_{fnt} = cross-sectional area of non-prestressing tendons at top of flange
A_{fu} = total cross-sectional area of unbonded post-tensioning tendons
A_p = cross-sectional area of precast DT-beam
A_{pb} = total cross-sectional area of bonded pretensioning tendons
A_{pn} = total cross-sectional area of bonded non-prestressing tendons in webs of beam
A_{pnf} = total cross-sectional area of non-prestressing tendons in flange of beam
a = depth of equivalent rectangular compression block
b = width of compression face of member
b_w = width of web
C_f = resultant compression force in flange of precast DT-beam
C_R = resultant compression force
C_t = resultant compression force in concrete topping
c.g.c = axis passing through the centroid of concrete cross section of DT-beam
c.g.p = axis passing through the center of gravity of resultant pretensioned force
d = distance of center of gravity of the resultant tension force from extreme compression fiber
$\bar{d}$ = distance of center of gravity of resultant compression force from extreme compression fiber
d_b = distance of centroid of non-prestressing tendons at bottom of flange from extreme compression fiber
d_f = total thickness of flange of beam
d_j = distance of centroid of bonded prestressing tendons of individual row from extreme compression fiber
d_m = distance of centroid of bottom bonded prestressing tendons (m-th row) from extreme compression fiber
d_t = distance of centroid of non-prestressing tendons at top of flange from extreme compression fiber
d_u = distance of centroid of unbonded post-tensioning tendons from extreme compression fiber
E_c = modulus of elasticity of precast concrete
E_{ct} = modulus of elasticity of concrete topping
E_f = modulus of elasticity of bonded tendon
E_{fn} = modulus of elasticity of non-prestressing tendons in webs
E_{fp} = modulus of elasticity of unbonded tendon
e_b = eccentricity of resultant pretensioning force from centroid of precast concrete cross section
e_{uc} = eccentricity of unbonded post-tensioning tendons from centroid of composite section
e_{up} = eccentricity of unbonded post-tensioning tendons from centroid of precast concrete cross section
F_{pbj} = resultant tensile force in bonded prestressing tendons of individual row
F_{pbm} = resultant tensile force in bonded bottom (m-th row) prestressing tendons
F_{pe} = total initial effective pretensioning and post-tensioning forces
F_{pnb} = resultant compression force in non-prestressing tendons at bottom of flange
F_{pnj} = resultant tensile force in non-prestressing tendons of individual row in webs
F_{pnk} = resultant tensile force in non-prestressing tendons of bottom row (k-th row) in webs
F_{pnt} = resultant compression force in non-prestressing tendons at top of flange
F_{post} = resultant effective post-tensioning force in unbonded tendons
F_{pre} = resultant effective pretensioning force in bonded tendons
F_{pu} = resultant tensile force in unbonded post-tensioning tendons
F_R = resultant of tensile forces in bonded and unbonded tendons
f_{bi} = total stress in equivalent tendon of particular material located at centroid of corresponding tendons at balanced condition
f_c = stress in concrete at extreme compression fiber in significantly under-reinforced beam
f'_c = specified compressive strength of precast concrete
f_{ct} = stress in concrete at extreme compression fiber in over-reinforced beam
f_{fu} = specified tensile strength of bonded prestressing tendons
f_{fun} = specified tensile strength of non-prestressing tendons in webs
f_{fup} = specified tensile strength of unbonded post-tensioning tendons
f_{pbb} = flexural stress in equivalent bonded prestressing tendon at balanced condition
f_{pbj} = total stress in bonded prestressing tendons of individual row
f_{pbm} = total stress in bottom prestressing tendons (m-th row)
f_{pbmi} = initial effective prestress in bottom bonded prestressing tendons (m-th row)
f_{pnb} = total stress in non-prestressing tendons at flange bottom
f_{pnbb} = total stress in equivalent non-prestressing tendon of webs at balanced condition
f_{pnfb} = total stress in equivalent non-prestressing tendon of flange at balanced condition
f_{pnj} = total stress in non-prestressing tendons of individual row in webs
f_{pnk} = total stress in non-prestressing tendons of bottom row (k-th row)
f_{pnt} = total stress in non-prestressing tendons at top of flange
f_{pu} = total stress in unbonded post-tensioning tendons
f_{pub} = flexural stress in equivalent unbonded tendon at balanced condition
f_r = modulus of rupture of concrete
$\sum_{j=1}^{m} F_{pi}$ = total initial effective prestressing forces in bonded pretensioning tendons
h_f = thickness of flange of DT-beam
h_j = distance of centroid of non-prestressing tendons of individual row in webs
h_k = distance of centroid of bottom non-prestressing tendons (k-th row)
h_t = thickness of concrete topping
I_c = moment of inertia of composite concrete cross section
I_{cr} = gross transformed moment of inertia of cracked section
I_{tr} = gross transformed moment of inertia of gross cross section
k = number of rows of non-prestressing tendons in webs of DT-beam
k_u = neutral axis depth coefficient
L = effective span of beam
L_u = horizontal distance between ends of post-tensioning strands
M = applied maximum moment due to service loads
M_{cr} = cracking moment capacity of section
M_D = maximum bending moment due to dead load
M_L = maximum bending moment due to live load
M_n = nominal moment capacity of section
$M_{required}$ = required moment capacity of section
M_u = design moment capacity of section
m = number of rows of bonded pretensioning tendons
N.A. = neutral axis of DT-beam section
n = depth to neutral axis from extreme compression fiber
P_{cr} = midspan load causing cracking of DT-beam
p = number of materials used for tension reinforcement
q = total number of bonded prestressing and non-prestressing tendon layers
S_b = section modulus corresponding to bottom extreme fiber of composite section
W = total midspan load
W_d = self weight of beam/unit length
y_{tc} = distance of centroid of composite cross section from top fiber
α, β = stress block factors
α_1, β_1 = stress block factors for rectangular section
α_2, β_2 = stress block factors for flanged section
α_i = ratio of total stress in equivalent tendon of particular material at balanced condition to specified strength of pretensioned tendon
δ = maximum midspan deflection of beam under service loads
δ_a = maximum midspan deflection of beam due to applied load
δ_d = maximum midspan deflection of beam due to dead load
δ_p = maximum midspan deflection of beam due to prestressing forces
$\Delta\varepsilon_{pu}$ = flexural strain in unbonded post-tensioning tendons
ε_{cu} = ultimate compression strain in concrete
ε_f = difference in ultimate rupture strain and initial prestressing strain of bottom pretensioning tendons
ε_{fbj} = flexural strain in bonded prestressing tendons of individual row
ε_{fbm} = flexural strain in the bonded prestressing tendons of bottom row (m-th row)

ε_{fu} = ultimate tensile strain capacity of bonded prestressing tendons
ε_{fun} = ultimate tensile strain capacity of non-prestressing tendons in webs
ε_{fup} = ultimate tensile strain capacity of unbonded tendons
ε_{pbj} = total strain in bonded prestressing tendons of individual row
ε_{pbji} = initial strain in bonded prestressing tendons of individual row
ε_{pbm} = total strain in bonded prestressing tendons of *m*-th row
ε_{pbmi} = initial strain in bonded prestressing tendons of *m*-th row
ε_{pnb} = total strain in non-prestressing tendons at bottom of flange
ε_{pnj} = total strain in non-prestressing tendons of individual row in webs
ε_{pnk} = total strain in non-prestressing tendons of bottom row (*k*-th row)
ε_{pnt} = total strain in non-prestressing tendons at top of flange
ε_{pu} = total strain in unbonded post-tensioning tendons
ε_{pui} = initial strain in unbonded post-tensioning tendons
ε_t = strain at top of beam at specific load stage
Ω = bond reduction coefficient for uncracked section
Ω_c = bond reduction coefficient for cracked section
Ω_u = bond reduction coefficient at ultimate
ϕ = strength reduction factor
ρ = reinforcement ratio
ρ_b = balanced reinforcement ratio
σ_{bp} = resultant prestress at extreme tension fiber of beam due to effective pretensioning and post-tensioning forces

REFERENCES

1. ACI Committee 440, "State-of-the-Art Report on Fiber Reinforced Plastic (FRP) Reinforcement for Concrete Structures (ACI 440R-96)," American Concrete Institute, Farmington Hills, Mich., 1996, 65 pp.

2. Grace, N. F., and Abdel-Sayed, G., "Ductility of Prestressed Concrete Bridges Using CFRP Strands," *Concrete International*, V. 20, No. 6, June 1998, pp. 25-30.

3. Grace, N. F., and Abdel-Sayed, G., "Behavior of Externally Draped CFRP Tendons in Prestressed Concrete Bridges," *PCI Journal*, V. 43, No. 5, Sept.-Oct. 1998, pp. 88-101.

4. Grace, N. F., "Response of Continuous CFRP Prestressed Concrete Bridges under Static and Repeated Loadings," *PCI Journal*, V. 45, No. 6, Nov.-Dec. 2000, pp. 84-102.

5. Grace, N. F., "Transfer Length of CFRP/CFCC Strands for Double-T Beams," *PCI Journal*, V. 45, No. 5, Sept.-Oct. 2000, pp. 110-126.

6. Grace, N. F.; Enomoto, S.; and Yagi, K., "Behavior of CFCC and CFRP Leadline Prestressing System in Bridge Construction," *PCI Journal*, V. 47, No. 3, May-June 2002, pp. 90-103.

7. Gerritse, A., and Werner, J., "ARAPREE—A Non-Metallic Tendon," *Advanced Composite Materials in Civil Engineering Structures*, ASCE, Materials Engineering Division, New York, 1991, pp. 143-154.

8. Dolan, C. W., "Kevlar Reinforced Prestressing for Bridge Decks," *Transportation Research Record 1290*, Third Bridge Engineering Conference, Denver, Colo., Mar. 1991, pp. 68-75.

9. Gilstrap, J. M.; Burke, C. R.; Dowden, D. M.; and Dolan, C. W., "Development of FRP Reinforcement Guidelines for Prestressed Concrete Structures," *Journal of Composites for Construction*, ASCE, V. 1, No. 4, Nov. 1997, pp. 131-139.

10. Dolan, C. W., and Burke, C. R., "Flexural Strength and Design of FRP Prestressed Beams," *Advanced Composite Materials in Bridges and Structures*, M. M. El-Badry, ed., Second International Symposium, Canadian Society for Civil Engineering, Montreal, Quebec, Canada, 1996, pp. 383-390.

11. Abdelrahman, A. A., and Rizkalla, S. H., "Serviceability of Concrete Beams Prestressed by Carbon Fiber-Reinforced Plastic Bars," *ACI Structural Journal*, V. 94, No. 4, July-Aug. 1997, pp. 447-457.

12. Burke, C. R., and Dolan, C. W., "Flexural Design of Prestressed Concrete Beams Using FRP Tendons," *PCI Journal*, V. 46, No. 2, Mar.-Apr. 2001, pp. 76-87.

13. Dolan, C. W., and Swanson, D., "Development of Flexural Capacity of a FRP Prestressed Beam with Vertically Distributed Tendons," *Proceedings*, ACUN-2, International Composites Conference, University of New South Wales, Sydney, Australia, Feb. 14-18, 2000, pp. 96-101.

14. Grace, N. F.; Enomoto, T.; Abdel-Sayed, G.; Yagi, K.; and Collavino, L., "Full-Scale Evaluation of CFRP/CFCC Prestressed DT-Beam." (accepted for publication in the *PCI Journal*)

15. Grace, N. F.; Navarre, F. C; Nacey, R. B.; Bonus, W.; and Collavino, L., "Design-Construction of Bridge Street Bridge—First CFRP Bridge in the United States," *PCI Journal*, V. 47, No. 5, Sept.-Oct. 2002, pp. 20-35.

16. Theriault, M., and Benmokrane, B., "Effects of FRP Reinforcement Ratio and Concrete Strength on Flexural Behavior of Concrete Beams," *Journal of Composites for Construction*, ASCE, V. 2, No. 1, Feb. 1998, pp. 7-16.

17. ACI Committee 318, "Building Code Requirements for Structural Concrete (ACI 318-99) and Commentary (318R-99)," American Concrete Institute, Farmington Hills, Mich., 391 pp.

18. Japan Society of Civil Engineers (JSCE), "Recommendation for Design and Construction of Concrete Structures Using Continuous Fiber Reinforcing Materials," Concrete Engineering Series 23, Research Committee on Continuous Fiber Reinforcing Materials, Tokyo, Japan, 1997, 325 pp.

19. American Association of State Highways and Transportation Officials (AASHTO), "LRFD Bridge Design Specifications," Washington, D.C., 1998.

20. Bakht, B.; Al-Bazi, G.; Banthia, N.; Cheung, M.; Erki, M. A.; Faoro, M.; Machida, A.; Mufti, A. A.; Neale, K. W.; and Tadros, G., "Canadian Bridge Design Code Provisions For Fiber-Reinforced Structures," *Journal of Composites for Construction*, ASCE, V. 4., No. 1, Feb. 2000, pp. 3-15.

21. Lin, T. Y., and Burns, N. H., *Design of Prestressed Concrete Structures*, 3rd Edition, John Wiley & Sons Publisher, New York, 1981, 656 pp.

22. Naaman, A. E., and Alkhairi, F. M., "Stress at Ultimate in Unbonded Post-Tensioning Tendons: Part 2—Proposed Methodology," *ACI Structural Journal*, V. 88, No. 6, Nov.-Dec. 1991, pp. 683-692.

23. CHBDC, "Canadian Highway Bridge Design Code," CAN/CSA-S6-00, CSA International, Toronto, Ontario, Canada, 2000.

24. Tan, K.-H.; Abdullah-Al Farooq, M.; and Ng, C.-K., "Behavior of Simple-Span Reinforced Concrete Beams Locally Strengthened with External Tendons," *ACI Structural Journal*, V. 98, No. 2, Mar.-Apr. 2001, pp. 174-183.

25. Mitsubishi Chemical Corp. (MCC), *Leadline™ Carbon Fiber Tendons/Bars*, Product Manual, Tokyo, Japan, 1994, 14 pp.

26. Tokyo Rope Mfg. Co. Ltd., *Technical Data on CFCC*, Product Manual, Tokyo, Japan, 1993, 100 pp.

27. NEFMAC, Technical Data Collection, Autocon Composite Inc., Canada, 1996, pp. 1-10.